

EDropout: Energy-Based Dropout and Pruning of Deep Neural Networks

Hojjat Salehinejad and Shahrokh Valaee, *Fellow, IEEE*

Abstract—Dropout is a well-known regularization method by sampling a sub-network from a larger deep neural network and training different sub-networks on different subsets of the data. Inspired by the dropout concept, we propose EDropout as an energy-based framework for pruning neural networks in classification tasks. In this approach, a set of binary pruning state vectors (population) represents a set of corresponding sub-networks from an arbitrary original neural network. An energy loss function assigns a scalar energy loss value to each pruning state. The energy-based model stochastically evolves the population to find states with lower energy loss. The best pruning state is then selected and applied to the original network. Similar to dropout, the kept weights are updated using backpropagation in a probabilistic model. The energy-based model again searches for better pruning states and the cycle continues. This procedure is in fact a switching between the energy model, which manages the pruning states, and the probabilistic model, which updates the kept weights, in each iteration. The population can dynamically converge to a pruning state. This can be interpreted as dropout leading to pruning the network. From an implementation perspective, despite most of the pruning methods, EDropout can prune neural networks without manually modifying the network architecture code. We evaluated the proposed method on different flavours of ResNets, AlexNet, and SqueezeNet on the Kuzushiji, Fashion, CIFAR-10, CIFAR-100, and Flowers datasets, and compared the pruning rate and classification performance of the models. The networks trained with EDropout on average achieved a pruning rate of more than 50% of the trainable parameters with approximately $< 5\%$ and $< 1\%$ drop of Top-1 and Top-5 classification accuracy, respectively.

Index Terms—Dropout, energy-based models, pruning deep neural networks.

I. INTRODUCTION

Deep neural networks (DNNs) have different learning capacities based on the number of trainable parameters for classification tasks. Depending on the complexity of the dataset (e.g. size of dataset and number of classes), selecting a network which maximizes the generalization performance often involves trial and error. DNNs with larger capacity often have better performance, but they take longer time to train, may suffer from lack of generalization, and have redundancy in trained parameters. Particularly for applications such as edge computing and embedded systems, smaller networks are more desirable since DNNs are computationally intensive, require large memory, and consume extensive energy [1]. Pruning DNNs is one of the major approaches to reducing the number

of trainable weights while maintaining the classification performance. Most of the proposed methods for deploying DNN on edge devices can be divided into pruning of existing large DNNs, or small networks by design. Our focus in this paper is on methods that can prune a given DNN.

Dropout [2], which was originally proposed as a regularization technique to train DNNs, reduces complexity of the network by randomly dropping a subset of the parameters in each training phase and fully utilizes the parameters (full network) for inference. Despite other regularization methods such as l_1 and l_2 norms [3], which modify the loss function, the dropout-based methods modify the network structure that is equivalent to training different smaller neural networks in each iteration. A variety of methods has been proposed for *smarter* dropout such as standout [4], variational dropout [5], and adversarial dropout [6]. Dropout is mainly proposed for dense layers while it is much less used in convolution layers. While dropout [2] sets a subset of activation values to zero, DropConnect [7] zeroes a randomly selected subset of weights in a fully connected network. A survey on dropout methods is provided in [8].

Pruning is different from dropout, where the trainable parameters are permanently dropped and is mainly used to remove redundant weights while preserving the classification accuracy. Removing inactive and redundant weights from a network can lead to a smaller network which improves generalization performance and faster inference of the network [9]. In general, pruning algorithms have three stages which are training, pruning, and fine-tuning [10]. One of the early attempts was to use second derivative information to minimize a cost function that reduces network complexity by removing excess number of trainable parameters and further training the remaining of the network to increase inference accuracy [9]. Soft weight-sharing [11] is another approach by clustering weights into subgroups with similar weight values. It adds a penalty term to the cost function of the network where the distribution of weight values is modeled as mixture of multiple Gaussians and the means and variance of clusters are adapted during the training of network [11]. This work has been further enhanced in [12]. *Deep Compression* has three stages that are pruning, quantization, and Huffman coding, which targets reducing the storage requirement of a DNN without affecting its accuracy [1]. This method works by pruning all connections with weights below a threshold followed by retraining the sparsified network.

The concept of energy has been used before for pruning DNNs, where we have proposed an Ising energy-based model for dropout and pruning of hidden units in multi-layer per-

H. Salehinejad and S. Valaee are with the Department of Electrical & Computer Engineering, University of Toronto, Toronto, Canada e-mail: hojjat.salehinejad@mail.utoronto.ca, valaee@ece.utoronto.ca.

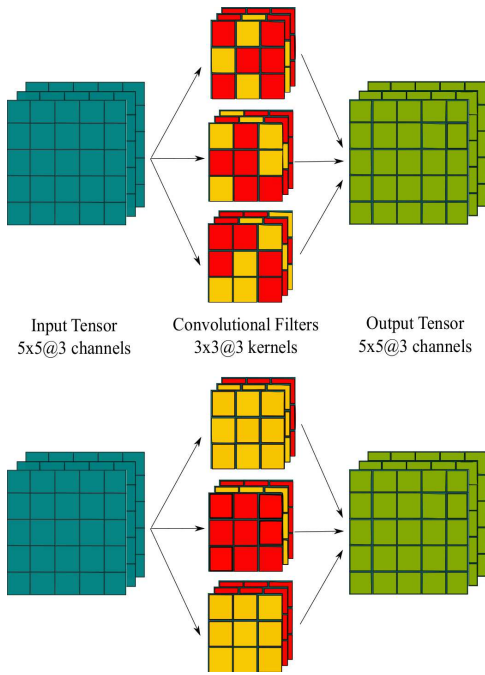


Fig. 1: Top: Unstructured pruning; Bottom: Structured pruning. Red elements are pruned.

ception (MLP) neural networks in [13]. In this approach, the network is modeled as a graph where each node is a hidden unit and the edge between nodes represents a measure of activation of each unit. We used a high-speed hardware to search for the best sub-network using Markov Chain Monte Carlo (MCMC) [14] method. Later, we scaled up this method for pruning large-scale MLPs using a node grouping technique [15].

In this paper, for the first time in the literature to best our knowledge, we introduce the concept of using energy-based models (EBMs) [16] for pruning of convolutional and dense layers. This method behaves as a hybrid technique, where similar to random dropout, it trains different sub-networks of the original DNN at a time, leading to a pruned network. The trained network is in fact a subset of the original network, which has a competitive performance to the network at full capacity but with a smaller number of parameters. We introduce utilizing a population of pruning candidate states, where each state vector in the population represents a set of active trainable weights from the network. Each vector has a corresponding energy loss value as a measure of dependency between sub-network parameters. The objective is to search for state vectors with lower energy loss. Indeed for a DNN with $|\Theta|$ number of trainable parameters, this is a combinatorial optimization problem which requires $2^{|\Theta|}$ times evaluation of the energy loss function for each batch of data. Since this procedure is NP-hard, we also propose a stochastic parallel binary technique based on the differential evolution (DE) [17] to search for the sparse state of the network. In this paper, our focus is to study and evaluate *EDropout* in pruning DNNs and not as a regularization method. Our results show on average more than 50% pruning of trainable network parameters while maintaining classification performance — the Top-1 and Top-

5 classification accuracy drop on average $< 5\%$ and $< 1\%$, respectively — on several image classification tasks with various number of classes and available training samples on ResNets, AlexNet, and SqueezeNet.

II. BACKGROUND

A. Pruning Methods

Pruning methods in neural networks can be divided into unstructured and structured methods. Figure 1 shows an illustration of these two approaches.

1) *Unstructured Pruning*: Unstructured pruning removes any subset of weights without following a specific geometry like the entire kernel, filter, or channel [18]. This kind of pruning results in a sub-network with geometrically sparse weights, which is difficult to implement in practice as a smaller network due to predefined tensor-based operations on graphical processing units (GPUs). It also requires overhead computation to address the location of kept weights. Therefore, it is difficult to get computational advantage from this approach. However, due to granular level of sparsity, this approach generally has lower drop of accuracy compared with the structured methods and the original model.

2) *Structured Pruning*: Structured pruning generally follows some constraints and defined structure in pruning a network. Typically pruning happens at channel, kernel, and intra-kernel levels. All the incoming and outgoing weights to/from a feature map are pruned in a channel level pruning which can result in an intensive reduction of network weights. In kernel level pruning, a subset of kernels is entirely pruned. In the intra-kernel level, the weights in a kernel can be pruned [18], for example a specific row or column. Compared with the unstructured pruning, the structured pruning has very little computational cost overhead and is easier to implement and scale on GPUs. The advantage is faster implementation and inference. A group of state-of-the-art structured pruning algorithms is examined in [10], which concludes that fine-tuning a pruned model only gives comparable or worse performance than training the model with randomly initialized weights.

B. Energy-based Models

In general, solving a classification problem using DNNs with C data classes $\mathcal{Y} = \{y_1, \dots, y_C\}$ is defined as using a parametric function to map the input $X \in \mathcal{X}$ to C real-valued numbers $\epsilon = \{\epsilon_1, \epsilon_2, \dots, \epsilon_C\}$ (a.k.a. logits). This function is in fact a stack of convolutional and dense layers with non-linear activation functions. The output is then passed to a classifier, such as *Softmax* function, which is a member of the *Gibbs distributions*, to parameterize a categorical distribution in form of a probability distribution over the data classes [19], defined as $\{p(y_1), \dots, p(y_C)\}$ where for simplicity we define $p_c = p(y_c) \forall c \in \{1, \dots, C\}$. The loss is then calculated based on cross-entropy with respect to the correct answer Y .

The Gibbs distribution (a.k.a the Boltzman distribution), which is a very general family of probability distributions, is defined as

$$p(Y|X) = \frac{e^{-\beta \mathcal{F}(Y,X)}}{Z(\beta)}, \quad (1)$$

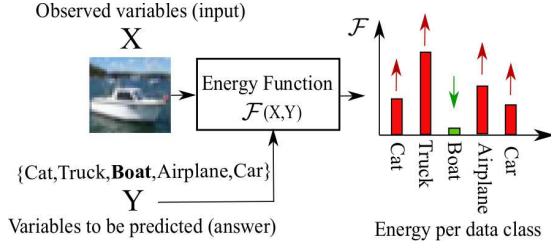


Fig. 2: Energy-based model (EBM), [16].

where $Z(\beta) = \sum_{y_c \in \mathcal{Y}} e^{-\beta \mathcal{F}(y_c, X)}$ is the partition function, $\beta > 0$ is the inverse temperature parameter [16], and $\mathcal{F}(\cdot)$ is referred to as *Hamiltonian* or the *energy function*. The Gibbs distribution naturally permits annealing, by changing the temperature during the training procedure [20]. β is discussed in [21] as the *distillation* where a higher value for $1/\beta$ produces a softer probability distribution over classes.

In general, some probabilistic models can be considered as a special type of EBMs. An EBM assigns a *scalar energy loss* as a measure of compatibility to a configuration of parameters in neural networks [16], as demonstrated in Figure 2. One of the advantages of this approach is avoiding normalization, which can be interpreted as an alternative to probabilistic estimation [16]. Calculating the exact probability in (1) needs computing the partition function over all the data classes C . However, for large C , such as in language models with more than 100,000 classes, this causes a bottleneck [22]. In addition, in order to follow the probability axioms, specifically $\sum_{c=1}^C p_c = 1$, the Softmax transfer function generates prior probability values that are close to zero for each class. Some methods such as annealed importance sampling [23] have been proposed to deal with this problem which is out of the scope of this paper.

C. Differential Evolution

Population-based optimization algorithms are popular methods for solving combinatorial high-dimensional optimization problems. The advantage of such methods is using a population of candidate solutions to search the problem landscape to minimize/maximize the objective function. DE is one of the popular and well-known population based algorithms. The search procedure starts with S initial candidate solutions (individuals) $\mathbf{S}^{S \times D}$ with dimension D and based on the scaled difference between two selected individuals $\mathbf{s}_i, \mathbf{s}_{j \neq i} \in \mathbf{S}$ improves the candidate solutions in each generation toward an optimal solution [24]. The standard version of DE for *continuous problems* has three major operations: mutation, crossover, and selection.

Mutation: For an individual $\mathbf{s}_i \in \mathbf{S}$, three different individuals $\mathbf{s}_{i_1}, \mathbf{s}_{i_2}$, and \mathbf{s}_{i_3} are selected from \mathbf{S} . The mutant vector of \mathbf{s}_i is then calculated as

$$\mathbf{v}_i = \mathbf{s}_{i_1} + F(\mathbf{s}_{i_2} - \mathbf{s}_{i_3}), \quad (2)$$

where the mutation factor $F \in (0.1, 1.5)$ is a real constant that controls the amplification of the added differential variation of

$\mathbf{s}_{i_2} - \mathbf{s}_{i_3}$. The exploration of DE increases by selecting higher values for F .

Crossover: The crossover operation increases diversity of the population by shuffling the mutant and parent vectors as

$$u_{i,d} = \begin{cases} v_{i,d}, & r'_d \leq C_r \text{ or } d_{rand} = d \\ s_{i,d}, & \text{otherwise} \end{cases}, \quad (3)$$

for all $d \in \{1, \dots, D\}$ and $i \in \{1, \dots, S\}$. $C_r \in [0, 1]$ is the crossover rate, $r'_d \in [0, 1]$, and d_{rand} is a random integer from the interval $[1, D]$.

Selection: The \mathbf{u}_i and \mathbf{s}_i vectors are evaluated for each $\mathbf{s}_i \in \mathbf{S}$ and compared with respect to their fitness value. The one with better fitness (lower value for minimization problem) is selected for the next generation.

The above procedures generally continues for a predefined number of generations or until some convergence criteria are satisfied.

III. ENERGY-BASED DROPOUT AND PRUNING

Figure 3 shows different steps of EDropout applied on a simple neural network with two convolutional layers, one hidden layer, and 10 data classes. For simplicity of visualizations, only the pruning on convolutional layers is presented to decrease the dimensionality of state vectors. First, we define the *pruning states* and the energy model of EDropout. Then, the training and optimization procedures are discussed as follows.

A. Pruning States

A given neural network has a set of trainable parameters Θ , which is generally a combination of parameters in convolutional and dense layers. In convolutional layers, we are interested in dropping weight kernels, and in dense layers the units, including their bias terms. A feature map in a convolutional layer is the output of convolving a weight kernel with the incoming activation values. Therefore, dropping a weight kernel can also be interpreted as dropping a feature map.

Let us define a set of S binary candidate pruning state vectors as the population $\mathbf{S}^{S \times D}$. Each vector $\mathbf{s}_i \in \mathbf{S}$ of length D represents the state of trainable kernels in a convolution layer and units in the dense layers, referred to as a *unit* hereafter for convenience. If $s_{i,d} = 0$ unit d is ignored (inactive) and if $s_{i,d} = 1$ it participates (active) during training and inference. Each state vector \mathbf{s}_i corresponds to a sub-network of the original network with the corresponding energy function values $\mathcal{F}_i \in \{\mathcal{F}_1, \dots, \mathcal{F}_S\}$, where generally we can have 2^D possible energy functions.

Step 1 of Figure 3 shows an example of the population of candidate pruning state vectors. Since the first convolutional layer has 4 kernels and the second one has 6 kernels, the length of each state vector is $D = 10$. So, if $s_{i,d} = 0$, the unit is inactive (white circle) and the corresponding weights are removed from the original network in Step 2. As an example given the last state vector \mathbf{s}_i with $i = S$, where $s_{i,d} = 0 \forall d \in \{3, 8, 9\}$, the corresponding weights are removed from the original network and illustrated as red

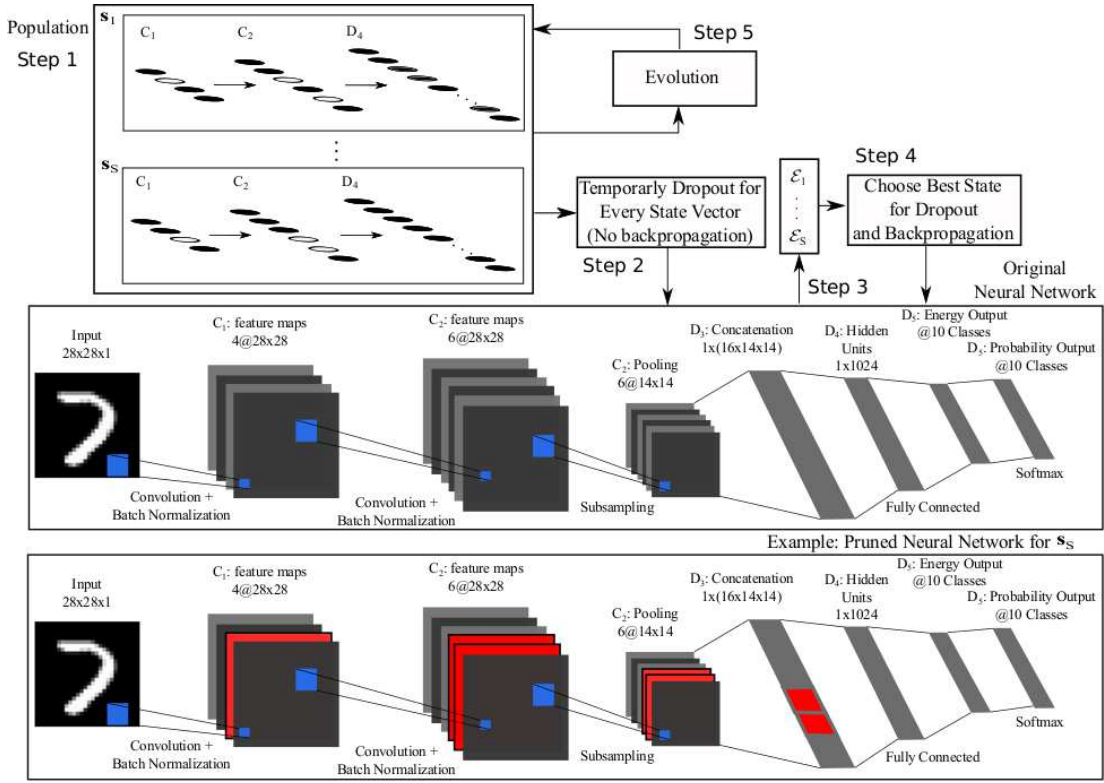


Fig. 3: Different steps of EDropout. Step 1: Population initialization; Step 2: Apply dropout to the network for each state vector; Step 3: Compute energy loss for each state vector; Step 4: Select the best state vectors based on the energy loss and perform dropout and then backpropagation (on kept weights only); Step 5: Evolve the population of candidate state vectors and continue to Step 1.

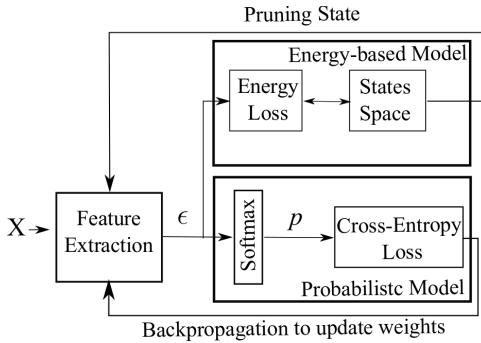


Fig. 4: Switching between the energy-based model (EBM) and the probabilistic model. The EBM searches for the pruning state and the probabilistic models searches for the weights. Both models are aware of target class Y during training. In inference, the best pruning state is applied and the EBM is removed.

units. Since two kernels are inactive in the last convolutional layer, the corresponding units are also inactive in the next concatenation layer.

B. Energy Model

The Gibbs distribution gives considerable flexibility in defining pruning methods [20]. For example, every Markov random field (MRF) corresponds to a Gibbs distribution, and vice versa. Gibbs distribution is a probability measure to define the state of a system (such as a DNN) based on the given *energy* of the system. Softmax function which is the

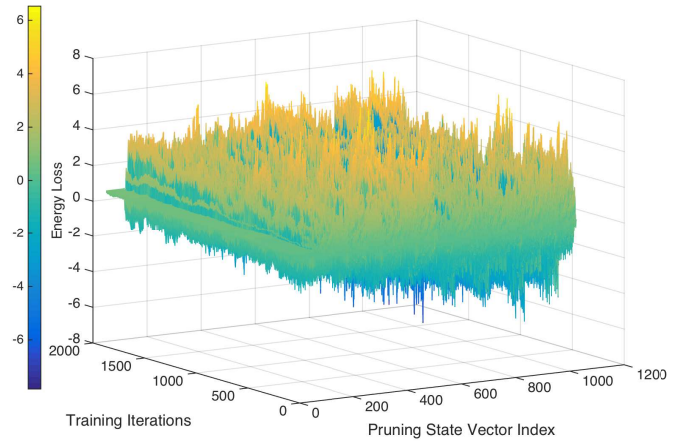


Fig. 5: Energy loss landscape for all possible pruning state vectors (2^D) during training iterations.

normalized exponential function generally used in training DNN for classification problems has the similar form as the Boltzman distribution [25]. An energy function is a measure of compatibility, which represents the dependencies of a subset of the network variables as a scalar energy, based on the definition of EBMs in [16].

By choosing $\beta = 1$ in the Gibbs distribution (1), the energy function corresponding to using a Softmax layer in training

Algorithm 1: EDropout

```

Set  $t = 0$  // Optimization counter
Initiate the neural network with trainable weights  $\Theta$ 
Set  $\mathbf{S}^{(0)} \sim \text{Bernoulli}(P = 0.5)$  // States initialization
Set  $\Delta s \neq 0$  &  $\Delta s_T$ 
for  $i_{epoch} = 1 \rightarrow N_{epoch}$  do // epoch counter
  for  $i_{batch} = 1 \rightarrow N_{batch}$  do // batch counter
     $t = t + 1$ 
    if  $\Delta s \neq 0$  or  $i_{epoch} \leq \Delta s_T$  then
      if  $i_{epoch} = 1$  &  $i_{batch} = 1$  then
        Compute energy loss of  $\mathbf{S}^{(0)}$  as  $\mathcal{E}^{(0)}$  using (7)
      end if
      for  $i = 1 \rightarrow S$  do // States counter
        Generate mutually different  $i_1, i_2, i_3 \in \{1, \dots, S\}$ 
        for  $d = 1 \rightarrow D$  do // State dimension counter
          Generate a random number  $r_d \in [0, 1]$ 
          Compute mutation vector  $v_{i,d}$  using (8)
          Compute candidate state  $\tilde{s}^{(t)}$  using (9)
        end for
      end for
      Compute energy loss of  $\tilde{\mathbf{S}}^{(t)}$  as  $\tilde{\mathcal{E}}^{(t)}$  using (7)
      Select  $\mathbf{S}^{(t)}$  and corresponding energy  $\mathcal{E}^{(t)}$  using (10)
      Select the state with the lowest energy from  $\mathbf{S}^{(t)}$  as  $\mathbf{s}_b^{(t)}$ 
    else
       $\mathbf{s}_b^{(t)} = \mathbf{s}_b^{(t-1)}$ 
    end if
    Temporarily drop weights of the network based on the best
    state  $\mathbf{s}_b^{(t)}$ 
    Compute loss of the sparsified network
    Perform backpropagation to update  $\Theta$ 
  end for
  Update  $\Delta s$  for early state convergence using (11)
end for

```

neural networks is given by

$$\mathcal{F}(Y, X) = -\epsilon, \quad (4)$$

where $\epsilon = [\epsilon_1, \dots, \epsilon_C]$. The Softmax function in training neural networks is defined as

$$p(y_c | X) = \frac{e^{\epsilon_c}}{\sum_{\epsilon_c \in \epsilon} e^{\epsilon_c}}. \quad (5)$$

Since Softmax is a special case of the Gibbs distribution, by setting $\beta = 1$ [25], and using the definition in (1) we have

$$p(y_c | X) = \frac{e^{-\mathcal{F}(y_c, X)}}{\sum_{y_c \in \mathcal{Y}} e^{-\mathcal{F}(y_c, X)}}, \quad (6)$$

where by comparing (1) and (6) we can interpret $\mathcal{F}(y_c, X) = -\epsilon_c$ and in a generalized form $\mathcal{F}(Y, X) = -\epsilon$ for all $\epsilon_c \in \epsilon$.

In EBMs, training a model refers to finding an energy function $\mathcal{F}(Y, X, \Theta)$ that minimizes the energy loss of the model by searching the weights space [16]. However, we define pruning as the searching for a binary state vector \mathbf{s} that prunes the network while minimizes the energy loss for fixed Y, X , and Θ in each iteration, defined as $\mathcal{F}(Y, X, \Theta, \mathbf{s})$. We are using the cross-entropy loss and back-propagation to search for the weights. Hence, the search for weights is conducted using a probabilistic model while the pruning state vector is fixed and the search for pruning state is conducted using an EBM while the weights are fixed in each iteration, as illustrated in Figure 4. Based on this concept, different energy functions can

be defined. The candidate states defined in Section III-A help to find a subset of the neural network and capture its energy function that associates low energies to correct values of the remaining variables, and higher energies to incorrect values.

We define the following energy loss function to measure the quality of energy function for (X, Y) with target output y_c as

$$\begin{aligned} \mathcal{E} &= \mathcal{L}(Y, \mathcal{F}) \\ &= \mathcal{F}(y_c, X) - \min\{\mathcal{F}(y_{c'}, X) : y_{c'} \in \mathcal{Y}, c' \neq c\}, \end{aligned} \quad (7)$$

where it can be extended for a batch of data. The *energy loss* function is intuitively designed to assign a low loss value to \mathcal{F}_s which has the lowest energy with respect to the target data class c and higher energy with respect to the other data classes and vice versa [16]. The corresponding energy loss values for the state vectors in Figure 3 are calculated in Step 3 as $[\mathcal{E}_1, \dots, \mathcal{E}_S]$.

Figure 5 shows the complexity of the energy loss landscape for a single input image and all possible state vectors (i.e. $2^D = 2^{10}$) over training iterations, which shows the problem is combinatorial with many possible local minima. In the next subsection, we discuss Steps 4 and 5 in Figure 3 to search for the best state vector in each training iteration on the energy landscape in Figure 5.

C. Training and Optimization

Training and optimization in EDropout has five main stages which are initialization, energy loss computation, energy loss optimization, early state convergence check, and training the sub-network in each iteration using back-propagation, as presented in Algorithm 1.

1) *Initialization*: At the beginning of training ($t = 0$), we initialize the candidate pruning states $\mathbf{S}^{(0)} \in \mathbb{Z}_2^{S \times D}$, where $s_{i,d}^{(0)} \sim \text{Bernoulli}(P = 0.5)$ for $i \in \{1, \dots, S\}$ and $d \in \{1, \dots, D\}$.

2) *Computing Energy Loss*: For each candidate state $\mathbf{s}_i^{(t)} \in \mathbf{S}^{(t)}$ in iteration t , the energy loss value is calculated using (7) as $\mathcal{E}_i^{(t)}$.

3) *Energy Loss Optimization*: Searching for the pruning state which can minimize the energy loss value is an NP-hard combinatorial problem. Various methods such as MCMC [26] and simulated annealing (SA) can be used to search for low energy states. We propose using a binary version of DE (BDE) [17] to minimize the energy loss function. This method has the advantage of searching the optimization landscape in parallel and sharing the search experience among candidate states. The other advantage of this approach is flexibility of designing the energy function with constraints.

The optimization step has three phases which are mutation, crossover, and selection. Given the population of states $\mathbf{S}^{(t-1)}$, a mutation vector is defined for each candidate state $\mathbf{s}_i^{(t-1)} \in \mathbf{S}^{(t-1)}$ as

$$v_{i,d} = \begin{cases} 1 - s_{i_1,d}^{(t-1)}, & \text{if } s_{i_2,d}^{(t-1)} \neq s_{i_3,d}^{(t-1)} \text{ \& } r_d < F \\ s_{i_1,d}^{(t-1)}, & \text{otherwise} \end{cases}, \quad (8)$$

for all $d \in \{1, \dots, D\}$, where $i_1, i_2, i_3 \in \{1, \dots, S\}$ are mutually different, F is the mutation factor [24], and $r_d \in [0, 1]$ is a

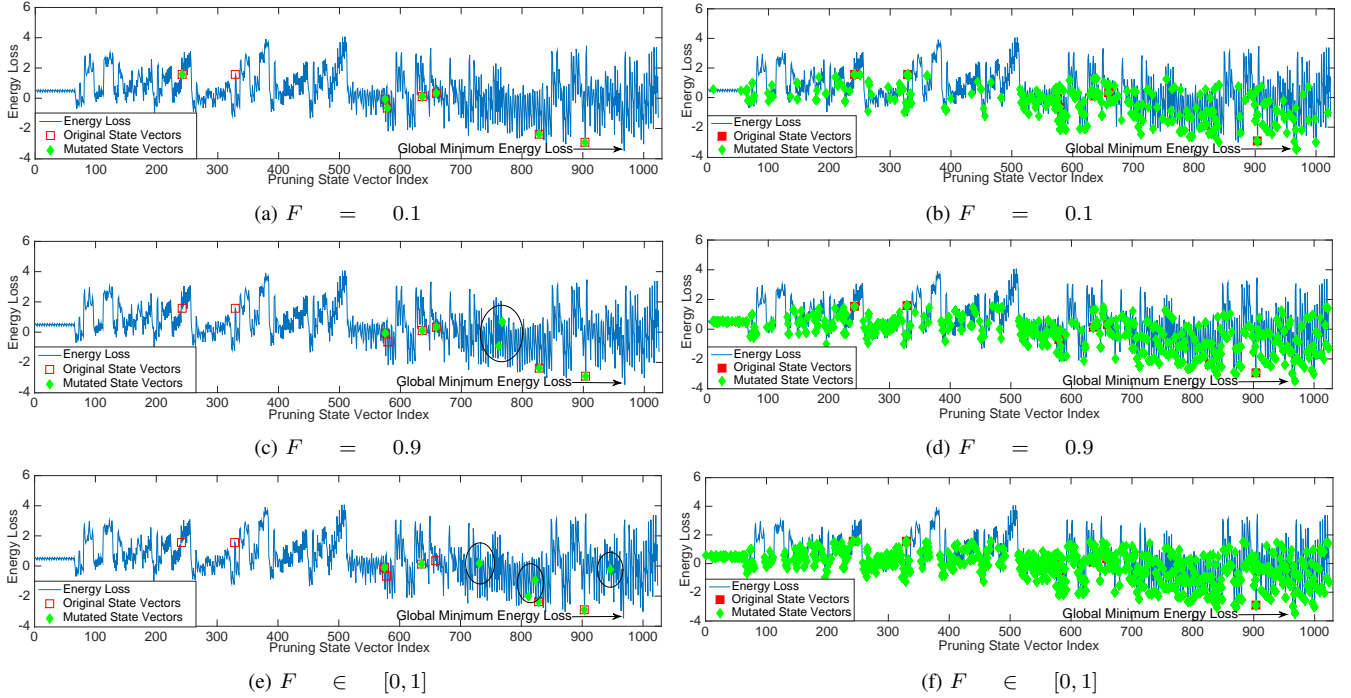


Fig. 6: Left: Visualization of mutated state vectors diversity in a single run. Right: Monte Carlo simulation of mutated state vectors diversity for 1,000 runs.

random number. The next step is to crossover the mutation vectors to generate new candidate state vectors as

$$\tilde{s}_{i,d}^{(t)} = \begin{cases} v_{i,d} & \text{if } r'_d \in [0, 1] \leq C_r \\ s_{i,d}^{(t-1)} & \text{otherwise} \end{cases}, \quad (9)$$

where C_r is the crossover coefficient [24]. The parameters C_r and F control exploration and exploitation of the population on the optimization landscape. Each generated state $\tilde{s}_i^{(t)}$ is then compared with its corresponding parent with respect to its energy loss value $\tilde{\mathcal{E}}_i^{(t)}$ as

$$\mathbf{s}_i^{(t)} = \begin{cases} \tilde{\mathbf{s}}_i^{(t)} & \text{if } \tilde{\mathcal{E}}_i^{(t)} \leq \mathcal{E}_i^{(t-1)} \\ \mathbf{s}_i^{(t-1)} & \text{otherwise} \end{cases} \quad \forall i \in \{1, \dots, S\}. \quad (10)$$

The state with minimum energy loss $\mathcal{E}_b^{(t)} = \min\{\mathcal{E}_1^{(t)}, \dots, \mathcal{E}_S^{(t)}\}$ is selected as the best state \mathbf{s}_b , which represents the sub-network for next training batch. This optimization strategy is simple and feasible to implement in parallel for a large S . Pre-defined number of active states can be defined in the optimizer to enforce a specific dropout/pruning rate.

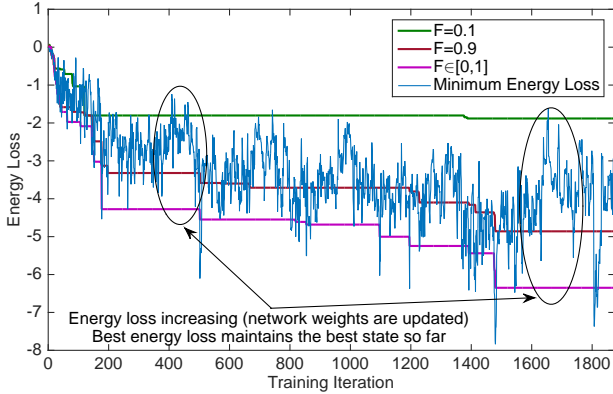
To better understand the importance of mutation factor, we select the energy loss landscape at iteration 1200 from Figure 5, where the state vector with lowest energy loss is $[1, 1, 1, 1, 0, 0, 0, 1, 1, 1]$ at index 968 with an energy loss value of -3.4715 . Then $S = 8$ random state vectors are initialized, as illustrated by red markers in Figures 6(a), 6(c), and 6(e) for $F = 0.1$, $F = 0.9$, and $F \in [0, 1]$, respectively, and $C_r = 0.9$. Then, the state vectors are mutated only once, their energy loss is compared with their parent, and the state vector with lower energy loss is denoted by green markers. The plots show $F = 0.9$ results in more diversity of mutated state vectors than

$F = 0.1$. We need to note that some mutated individuals may overlap, as for occurred for $F = 0.1$ and $F = 0.9$. If we use a random $F \in [0, 1]$, the diversity is further enhanced than using a constant F and mutated states are more likely to have a lower energy loss value than their parent. In another visualization, we perform a Monte Carlo simulation of the above experiment with 1,000 independent runs. Comparing Figures 6(b), 6(d), and 6(f) shows that $F \in [0, 1]$ has more exploration capability. In fact, for $F = 0.1$, $F = 0.9$, and $F \in [0, 1]$, 23.05%, 36.91%, and 60.35% of the possible states are visited, respectively.

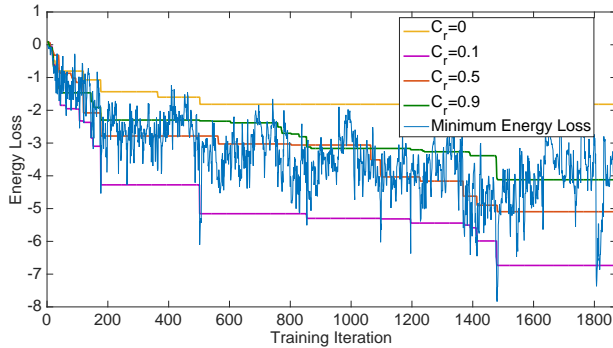
We also look at the energy loss landscape from the training iterations perspective. As Figure 7(a) shows, using the random $F \in [0, 1]$ results in better exploration of the optimization landscape, and ultimately, lower energy loss over the training iterations. It is interesting to observe that although the minimum energy loss values of a single input fluctuates during training (due to backpropagation on all training samples), but the energy loss of selected state vectors remains lowest possible so far (in terms of iterations) and enforces pruning while decreasing the overall energy loss.

The last visualization is about importance of the crossover rate, as illustrated in Figure 7(b) using $F \in [0, 1]$. We can observe that combination of mutation factor and crossover rate can control the exploration and exploitation of the search. Too much diversity ($F \in [0, 1]$ and $C_r = 0.9$) results in stagnation while a balance of these two parameters ($F \in [0, 1]$ and $C_r = 0.1$), can result in finding the states with lower energy loss.

4) *Early State Convergence*: The population-based optimizers are global optimization methods which generally converge to a locally optimal solution [27]. These algorithms suffer from premature convergence and stagnation problems.



(a) Convergence of best mutated state vector for different mutation factors with $C_r = 0.5$.



(b) Convergence of best mutated state vector for different crossover rates with $F \in [0, 1]$.

Fig. 7: Convergence of best mutated state vector for different mutation factors and crossover rates.

The former generally occurs when the population (candidate state vectors) has converged to local optima, has lost its diversity, or has no improvement in finding better solutions. The latter happens mainly when the population stays diverse during training [27].

The optimization process can run for every epoch of the neural network training. However, after a number of iterations, depending on the capacity of the neural network and the complexity of the dataset, all the states in $\mathbf{S}^{(t)}$ may converge to a state $s_b \in \mathbf{S}^{(t)}$. We call this the *early state convergence* phase and define it as

$$\Delta \mathbf{s} = \mathcal{E}_b^{(t)} - \frac{1}{S} \sum_{j=1}^S \mathcal{E}_j^{(t)}, \quad (11)$$

where $\mathcal{E}_b^{(t)}$ is the energy loss of s_b . So if $\Delta \mathbf{s} = 0$ we can call for an early state convergence and continue training by fine-tuning the sub-network identified by the state vector s_b . In addition, a stagnation threshold Δs_T is implemented where if $\Delta \mathbf{s} \neq 0$ after Δs_T number of training epochs, it stops the energy loss optimizer. These mechanisms are implemented to balance exploration and exploitation of the optimizer and address potential stagnation and premature convergence scenarios during training, as analyzed in Section IV-C1.

Most pruning and compression models first prune and train the network and then fine-tune it. The convergence to the

best state s_b in *EDropout* breaks the training procedure of the neural network into two phases. The first phase is when various subsets of the neural network, with potential overlap of units, are trained, which occurs before the convergence, and the second phase is when only a subset of network, chosen by s_b , is fine-tuned. The first phase is equivalent to training a network with *dropout*, which may act as a regularization method, and the second phase acts as *pruning* where the units/kernels are not trained anymore and are practically eliminated from the network. This leads to a *sparsified* neural network. Training the sparsified network is similar to a typical training of DNNs with back-propagation.

5) *Training*: Once the best candidate state is selected in each iteration, the state vector is applied to the network to compute the training loss. The back-propagation is then performed for the active units.

IV. EXPERIMENTS

We have performed extensive experiments on datasets with different level of difficulty and number of samples on several DNNs with different sizes and capacities. First, we analyze the parameters of the *EDropout* method and then discuss the performance results¹.

A. Data

The following benchmark datasets are used: (i) Fashion (gray images in 10 classes, 54k train, 6k validation, and 10k test) [28], (ii) Kuzushiji (gray images in 10 classes, 54k train, 6k validation, and 10k test) [29]; (iii) CIFAR-10 (color images in 10 classes, 45k train, 5k validation, and 10k test) [30], (iv) CIFAR-100 (color images in 100 classes, 45k train, 5k validation, and 10k test) [30], and (v) Flowers (102 flower categories; each class has between 40 and 258 images; 10 images from each class for validation and 10 for test) [31]. The horizontal flip and Cutout [32] augmentation methods are used for training on CIFAR and Flowers datasets. Input images are resized to 32×32 for ResNets and 224×224 for AlexNet [33] and SqueezeNet v1.1 [34].

B. Training Setup

The experiments are conducted on ResNets (18, 34, 50, and 101 layers) [35], AlexNet [33], SqueezeNet v1.1 [34], and Deep Compression [1]. The results are averaged over five independent runs. A grid hyper-parameter search is conducted based on the Top-1 accuracy for all models, including initial learning rates in $\{0.01, 0.1, 1\}$, Stochastic Gradient Descent (SGD) [36] and Adadelta [37] optimizer, exponential and step learning rate decays with gamma values in $\{25, 50\}$, and batch sizes of 64 and 128. The Adadelta optimizer with Step adaptive learning rate (step: every 50 epoch at gamma rate of 0.1) and weight decay of $10e^{-6}$ is used. The number of epochs is 200 and the batch size is 128. Random dropout is not used in the *EDropout* experiments. For the other models, where applicable, the random dropout rate is set to 0.5. The early

¹The codes and more details of experiments setup is available at: <https://github.com/sparsifai/edropout>

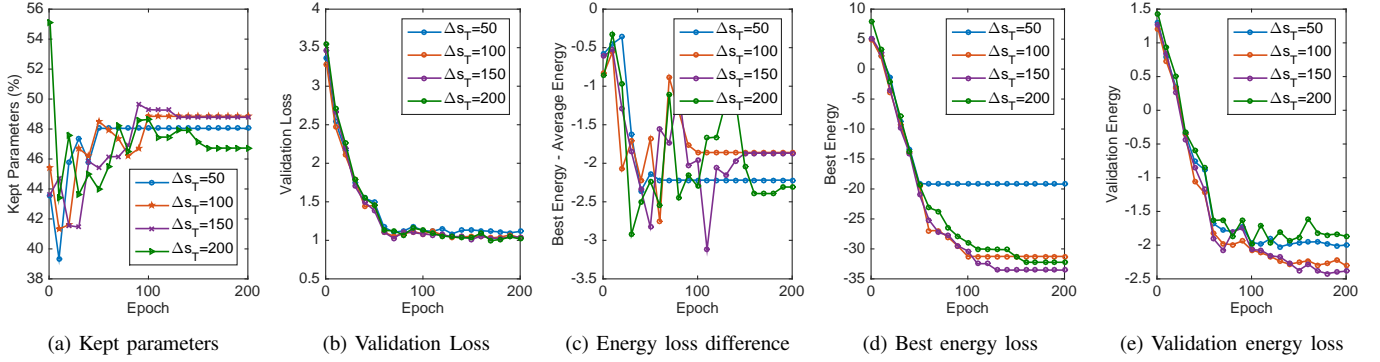


Fig. 8: Convergence of **ResNet-18** on **Flowers** validation dataset with $S = 8$ and initialization probability of $P = 0.5$ over 200 epochs.

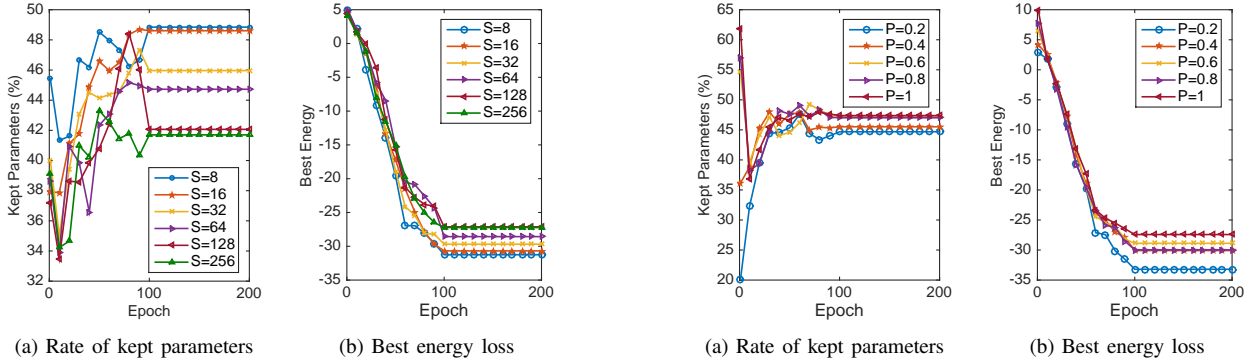


Fig. 9: Number of candidate state vectors analysis of **EDropout** for **ResNet-18** and **Flowers** dataset.

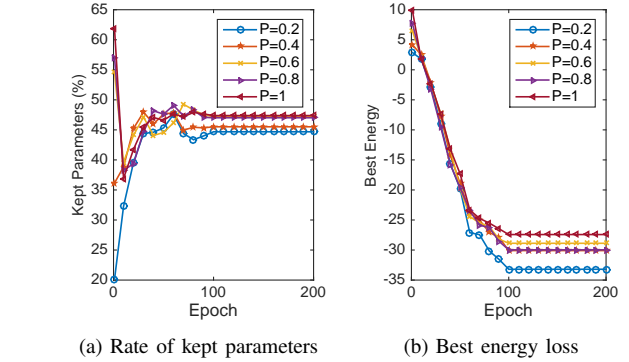


Fig. 10: States initialization analysis of **EDropout** for **ResNet-18** and **Flowers** dataset.

state convergence in (11) is used with a threshold of 100 epochs. The models are implemented in PyTorch [38] and trained on three NVIDIA Titan RTX GPUs.

C. Exploration vs. Exploitation: Dropout Leading to Pruning

The balance between exploration and exploitation in finding the best state vector is crucial. Number of candidate state vectors, initialization of the states, mutation factor, and cross-over rate are among the major parameters to control diversity of search.

1) *Early State Convergence*: Balancing the exploration of optimizer for a feasible state vector while giving enough time for fine-tuning that state is crucial. However, **EDropout** combines the state selection and training in the first phase and ultimately can naturally converge to a best state based on the energy of the states or manually be controlled with Δs_T . Figure 8(a) shows convergence of the kept number of parameters for $\Delta s_T \in \{50, 100, 150, 200\}$. For $\Delta s_T = 150$ and $\Delta s_T = 200$ the model has converged approximately at epochs 125 and 160, respectively. Figure 8(c) shows the value of Δs defined in (11), where as $|\Delta s| \rightarrow 0$ suggests the algorithm is moving toward exploitation (less diversity of candidate states) and as $|\Delta s| \rightarrow \infty$ it is moving toward exploration of the optimization landscape (more diversity of candidate states). This shows importance of using Δs_T as an added *early state convergence* metric, since even-though $\Delta s_T = 200$ has achieved a smaller number of parameters at approximately epoch 160, it decreases the chance of fine-tuning in the remaining epochs, resulting in an increase in

TABLE I: Performance study of **ResNet-18** on the **Flowers** dataset for different early state convergence thresholds Δs_T .

Δs_T	Loss	Top-1	Top-3	Top-5	R
50	1.7867	55.55	77.59	83.78	48.04
100	1.6550	61.54	79.18	85.55	48.19
150	1.8088	55.55	74.86	82.12	48.78
200	1.6853	57.31	75.73	82.89	46.72

TABLE II: Performance study of **ResNet-18** on the **Flowers** dataset for different number of candidate states S .

S	Loss	Top-1	Top-3	Top-5	R
8	1.6550	61.54	79.18	85.55	48.19
16	1.8029	55.93	75.74	81.92	48.60
32	1.7523	56.45	76.43	82.91	45.96
64	1.7248	57.20	77.69	83.97	44.72
128	1.7163	57.50	76.72	82.80	42.06
256	1.7042	58.12	77.62	83.69	41.69

TABLE III: Performance study of **ResNet-18** on the **Flowers** dataset for different states initialization probability P .

P	Loss	Top-1	Top-3	Top-5	R
0.2	1.6905	60.45	78.51	84.58	44.68
0.4	1.6776	59.39	77.60	83.80	46.25
0.6	1.7209	59.38	77.42	83.40	47.19
0.8	1.7084	58.97	77.70	83.97	47.31
1	1.6401	59.66	78.01	84.58	47.38

TABLE IV: Classification performance on test datasets. R is kept trainable parameters and $\#p$ is approximate number of trainable parameters. All the values except loss and $\#p$ are in percentage. (F) refers to full network used for inference and (P) refers to pruned network using *EDropout*.

(a) Kuzushiji							(b) Fashion						
Model	Loss	Top-1	Top-3	Top-5	R	$\#p$	Model	Loss	Top-1	Top-3	Top-5	R	$\#p$
ResNet-18	0.0709	98.23	99.53	99.79	100	11.1M	ResNet-18	0.2786	93.87	99.39	99.68	100	11.1M
ResNet-18+DeepCompression	0.1617	95.92	98.91	99.58	51.49	5.7M	ResNet-18+DeepCompression	0.2299	91.97	99.32	99.86	50.43	5.6M
ResNet-18+EDropout(F)	0.1112	97.75	99.41	99.78	100	11.1M	ResNet-18+EDropout(F)	0.4000	93.45	99.04	99.47	100	11.1M
ResNet-18+EDropout(P)	0.1107	97.78	99.45	99.73	51.49	5.7M	ResNet-18+EDropout(P)	0.3934	93.57	99.06	99.47	50.43	5.6M
ResNet-34	0.0704	99.52	99.90	99.93	100	21.2M	ResNet-34	0.3198	93.61	99.12	99.62	100	21.2M
ResNet-34+DeepCompression	0.2023	94.42	98.66	99.55	46.11	9.8M	ResNet-34+DeepCompression	0.2632	90.62	99.26	99.87	46.94	9.9M
ResNet-34+EDropout(F)	0.1115	97.78	99.42	99.72	100	21.2M	ResNet-34+EDropout(F)	0.4674	92.80	98.78	99.35	100	21.2M
ResNet-34+EDropout(P)	0.1143	97.71	99.44	99.65	46.11	9.8M	ResNet-34+EDropout(P)	0.4582	92.57	98.68	99.35	46.94	9.9M
ResNet-50	0.0902	97.70	99.44	99.79	100	23.5M	ResNet-50	0.3187	93.34	99.15	99.60	100	23.5M
ResNet-50+DeepCompression	0.2142	94.36	98.53	99.36	45.57	10.7M	ResNet-50+DeepCompression	0.2956	89.22	98.95	99.79	45.14	10.6M
ResNet-50+EDropout(F)	0.1250	97.89	99.38	99.75	100	23.5M	ResNet-50+EDropout(F)	0.5451	92.91	98.70	99.34	100	23.5M
ResNet-50+EDropout(P)	0.1289	97.63	99.35	99.73	45.57	10.7M	ResNet-50+EDropout(P)	0.5154	92.97	98.79	99.33	45.14	10.6M
ResNet-101	0.0699	98.26	99.63	99.80	100	42.5M	ResNet-101	0.3208	93.31	99.10	99.63	100	42.5M
ResNet-101+DeepCompression	0.5648	93.30	98.48	99.39	46.00	19.5M	ResNet-101+DeepCompression	1.4812	89.94	98.72	99.46	45.19	19.2M
ResNet-101+EDropout(F)	0.1140	98.06	99.39	99.69	100	42.5M	ResNet-101+EDropout(F)	0.5785	92.58	98.83	99.40	100	42.5M
ResNet-101+EDropout(P)	0.1087	98.05	99.47	99.69	46.00	19.5M	ResNet-101+EDropout(P)	0.5717	92.57	98.82	99.35	45.19	19.2M
AlexNet	0.1162	97.77	99.43	99.85	100	57M	AlexNet	0.4441	92.87	99.27	99.70	100	57M
AlexNet+EDropout(F)	0.1976	96.53	99.25	99.72	100	57M	AlexNet+EDropout(F)	0.3726	91.21	99.25	99.87	100	57M
AlexNet+EDropout(P)	0.2089	96.57	99.24	99.68	78.57	44.8M	AlexNet+EDropout(P)	0.3862	91.19	99.21	99.86	77.58	44.2M
SqueezeNet	0.2114	97.19	99.27	99.72	100	0.72M	SqueezeNet	0.3655	92.64	99.48	99.90	100	0.72M
SqueezeNet+EDropout(F)	0.2414	96.45	99.05	99.57	100	0.72M	SqueezeNet+EDropout(F)	0.2524	92.25	99.35	99.89	100	0.72M
SqueezeNet+EDropout(P)	0.2411	96.35	98.91	99.54	49.86	0.36M	SqueezeNet+EDropout(P)	0.2478	92.34	99.42	99.88	52.83	0.38M
(c) CIFAR-10							(d) CIFAR-100						
Model	Loss	Top-1	Top-3	Top-5	R	$\#p$	Model	Loss	Top-1	Top-3	Top-5	R	$\#p$
ResNet-18	0.3181	92.81	98.78	99.49	100	11.2M	ResNet-18	1.3830	69.03	84.44	88.90	100	11.2M
ResNet-18+DeepCompression	0.6951	76.15	94.16	98.59	49.66	5.5M	ResNet-18+DeepCompression	2.3072	40.01	62.20	72.28	48.04	5.4M
ResNet-18+EDropout(F)	0.4906	90.96	98.33	99.60	100	11.2M	ResNet-18+EDropout(F)	1.9479	67.04	84.11	89.43	100	11.2M
ResNet-18+EDropout(P)	0.4745	90.96	98.40	99.58	49.66	5.5M	ResNet-18+EDropout(P)	1.9541	67.06	84.14	89.27	48.04	5.4M
ResNet-34	0.3684	92.80	98.85	99.71	100	21.3M	ResNet-34	1.3931	69.96	85.65	90.10	100	21.3M
ResNet-34+DeepCompression	1.057	66.51	91.40	97.68	38.83	8.3M	ResNet-34+DeepCompression	2.1778	42.09	65.01	74.31	49.41	10.5M
ResNet-34+EDropout(F)	0.4576	88.28	97.47	99.31	100	21.3M	ResNet-34+EDropout(F)	1.9051	64.50	81.38	86.87	100	21.3M
ResNet-34+EDropout(P)	0.4598	88.21	97.48	99.28	38.83	8.3M	ResNet-34+EDropout(P)	1.9219	64.79	81.28	86.74	49.41	10.5M
ResNet-50	0.3761	92.21	98.70	99.51	100	23.5M	ResNet-50	1.3068	71.22	86.47	90.74	100	23.7M
ResNet-50+DeepCompression	1.0271	67.53	89.92	96.30	46.39	10.9M	ResNet-50+DeepCompression	2.3115	43.87	67.02	76.26	46.01	10.9M
ResNet-50+EDropout(F)	0.6041	85.22	96.35	98.77	100	23.5M	ResNet-50+EDropout(F)	1.8750	61.60	79.52	85.45	100	23.7M
ResNet-50+EDropout(P)	0.5953	85.30	96.62	98.76	46.39	10.9M	ResNet-50+EDropout(P)	1.8768	61.91	79.99	85.87	46.01	10.9M
ResNet-101	0.3680	92.66	98.69	99.65	100	42.5M	ResNet-101	1.3574	71.19	85.54	90.00	100	42.6M
ResNet-101+DeepCompression	1.037	66.32	92.65	98.11	45.10	19.2M	ResNet-101+DeepCompression	2.6003	37.08	58.78	68.76	43.76	18.6M
ResNet-101+EDropout(F)	0.6231	86.97	97.42	99.24	100	42.5M	ResNet-101+EDropout(F)	1.9558	61.52	79.71	85.20	100	42.6M
ResNet-101+EDropout(P)	0.6339	86.57	97.37	99.20	45.10	19.2M	ResNet-101+EDropout(P)	1.9412	61.92	79.49	85.23	43.76	18.6M
AlexNet	0.9727	84.32	96.58	99.08	100	57.4M	AlexNet	2.8113	60.12	79.18	83.31	100	57.4M
AlexNet+EDropout(F)	0.7632	75.05	93.74	98.18	100	57.4M	AlexNet+EDropout(F)	2.4731	56.62	78.72	81.92	100	57.4M
AlexNet+EDropout(P)	0.7897	74.66	93.63	97.96	77.36	44.4M	AlexNet+EDropout(P)	2.4819	56.59	78.52	81.62	71.84	41.2M
SqueezeNet	0.5585	81.49	96.31	99.01	100	0.73M	SqueezeNet	1.4150	67.85	85.81	89.69	100	0.77M
SqueezeNet+EDropout(F)	0.6686	76.76	94.55	98.62	100	0.73M	SqueezeNet+EDropout(F)	1.5265	64.23	82.71	88.63	100	0.77M
SqueezeNet+EDropout(P)	0.6725	76.85	95.00	98.56	52.35	0.38M	SqueezeNet+EDropout(P)	1.5341	64.02	81.63	88.51	56.40	0.43M
(e) Flowers													
Model	Loss	Top-1	Top-3	Top-5	R	$\#p$							
ResNet-18	1.8262	62.60	80.64	86.92	100	11.2M							
ResNet-18+DeepCompression	2.4988	53.92	60.68	76.38	48.19	5.4M							
ResNet-18+EDropout(F)	1.6808	58.73	77.19	82.40	100	11.2M							
ResNet-18+EDropout(P)	1.6550	61.54	79.18	85.55	48.19	5.4M							
ResNet-34	1.8993	63.22	81.08	87.16	100	21.3M							
ResNet-34+DeepCompression	2.4240	52.55	77.54	81.46	42.79	9.1M							
ResNet-34+EDropout(F)	1.6088	63.96	79.95	85.64	100	21.3M							
ResNet-34+EDropout(P)	1.5960	64.19	80.19	85.58	42.79	9.1M							
ResNet-50	2.4766	63.75	80.24	87.21	100	23.7M							
ResNet-50+DeepCompression	3.0556	27.28	47.43	57.63	44.68	10.6M							
ResNet-50+EDropout(F)	1.8492	54.60	76.46	82.84	100	23.7M							
ResNet-50+EDropout(P)	1.8293	56.02	76.42	83.10	44.68	10.6M							
ResNet-101	2.6183	62.70	82.04	86.26	100	42.7M							
ResNet-101+DeepCompression	3.0623	28.36	46.78	56.32	44.85	19.2M							
ResNet-101+EDropout(F)	1.8241	59.44	79.02	85.67	100	42.7M							
ResNet-101+EDropout(P)	1.8575	58.17	78.32	85.10	44.85	19.2M							
AlexNet	2.6872	56.11	74.85	81.92	100	57.4M							
AlexNet+EDropout(F)	2.5272	51.54	70.78	80.92	100	57.4M							
AlexNet+EDropout(P)	2.5159	51.79	71.12	80.67	81.12	46.5M							
SqueezeNet	2.2842	45.11	63.66	72.51	100	0.77M							
SqueezeNet+EDropout(F)	2.2217	42.76	62.90	72.02	100	0.77M							
SqueezeNet+EDropout(P)	2.2128	42.89	62.80	72.90	74.48	0.57M							

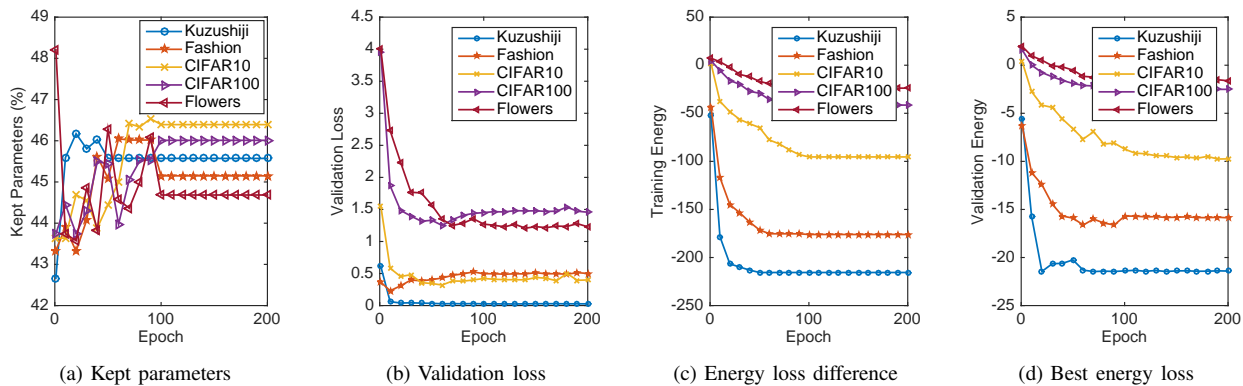


Fig. 11: Analysis of *EDropout* with **ResNet-50** on the validation dataset of Kuzushiji, Fashion, CIFAR-10, CIFAR-100 and Flowers datasets with $S = 8$, initialization probability of $P = 0.5$, and $\Delta s_T = 100$.

TABLE V: Inference time per image for batch size of 128 in seconds.

■ E-6 ■ E-5 ■ E-4 ■ E-3

Model	Original	EDropout S=8	EDropout S=32	EDropout Parallel S=8	EDropout Parallel S=32
ResNet-18	2.24E-5	1.30E-4	5.00E-4	3.25E-5	5.10E-5
ResNet-34	3.90E-5	2.40E-4	9.40E-4	6.86E-5	8.55E-5
ResNet-50	5.50E-5	3.40E-4	1.30E-3	8.95E-5	1.40E-4
ResNet-101	1.00E-4	6.00E-4	2.50E-3	1.70E-4	2.02E-4
AlexNet	7.34E-6	3.71E-5	1.30E-4	8.83E-6	9.54E-6
SqueezeNet	5.98E-5	2.20E-4	8.50E-4	6.90E-5	7.50E-5

the validation energy as plotted in Figure 8(e). Since we are minimizing the energy, it is obvious that $\Delta s_T \leq 0$ is guaranteed in (5). The interesting observation is pre-mature convergence of $\Delta s_T = 50$ and over-fitting of $\Delta s_T = 200$ in terms of best energy and validation energy in Figures 3(d) and 3(e). The results in Table I suggest $\Delta s_T = 100$ is a good threshold, since it has the highest Top-1 accuracy and also fairly splits half of the training budget for exploring and the other half for fine-tuning. This threshold is used for the rest of the experiments.

2) *Number of Candidate State Vectors*: A large number of candidate state vectors (i.e. the population size) S increases the exploration of the optimization landscape and meanwhile the stagnation risk. This is while a small population ($S \leq 8$, [24]) size encourages exploitation and fine-tuning of optimization. Different methods have been proposed to control this parameter. It has been shown in [24] that it is possible to maintain a high exploration capability while using a small population size by using a vectorized-random mutation factor (VRMF) trick. To analyze S , we trained ResNet-18 using *EDropout* for $S \in \{8, 16, 32, 64, 128, 256\}$ and the Flowers dataset. Table II shows that the small population size $S = 8$ and diversified with VRMF has achieved the best Top-1 score. However, larger S results in more pruning rate at a lower loss value. Figure 9 shows the rate of kept parameter and the best energy of the model during training epochs on the validation dataset, where $\Delta s_T = 100$. The plots show that smaller S converges faster to a lower energy while larger S has slower progress and is more prone to stagnation. Since the results show very competitive performance between various values of S , we use $S = 8$ for the rest of the experiments.

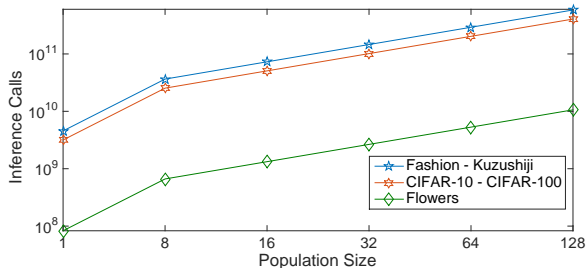
3) *States Initialization*: The probability P in $s_{i,d}^{(0)} \sim \text{Bernoulli}(P)$ governs the number of dropped/pruned trainable parameters for each state vector i at the initialization stage. If a specific pruning rate is desired, it is possible to define constraints in the evolution phase. Figure 10 shows convergence of ResNet-18 with *EDropout* using $P \in \{0.2, 0.4, 0.6, 0.8, 1\}$ on the Flowers validation dataset and the corresponding classification results on the test dataset is in Table III. The results show that at the beginning of training there is diversity in the number of kept parameters but the plots converge to a number in the range of [45%, 48%]. However, this affects the best energy, where the model with smaller P converges to lower energy. Since the results show small sensitivity of the models to P and convergence to approximately 50% pruning rate, P is set to 0.5 for fair binary distribution.

D. Classification Performance

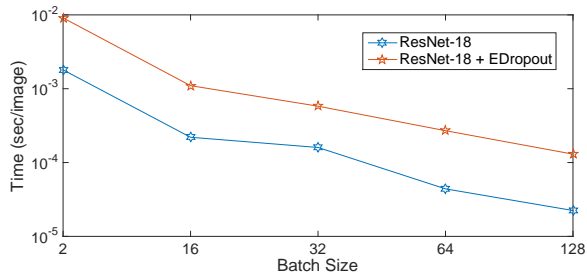
Table IV shows the classification performance results and Figure 11 shows convergence plots on the all validation dataset for ResNet-50 with *EDropout* as an example. The original models contain the entire trainable parameters and have larger learning capacity. *EDropout* in pruned and full versions have slightly lower Top-1 performance than the original model and competitive performance in terms of Top-5 performance. The Deep Compression [1] method receives pruning rate as input. For the sake of comparison, we have modified it to perform pruning on every convolution layer, given the rate achieved by *EDropout*, where generally it has lower performance than *EDropout*. SqueezeNet [39] is a small network with AlexNet level accuracy. *EDropout* is also applied to AlexNet and SqueezeNet v1.1, where it has a less pruning rate for AlexNet compared to ResNets but can prune approximately half of the trainable parameters in SqueezeNet v1.1 and achieve slightly lower performance.

E. Computational Complexity

The main drawback of *EDropout* is its computational complexity as a result of using a population of state vectors in the optimization phase to prune a network. In the worst-case scenario (i.e. without considering the early state convergence),



(a) Upper boundary of number of inference calls for different population sizes S and different number of training samples (the datasets in one line of legend have similar number of training samples). The Inference Calls axis is log scaled.



(b) Inference time of ResNet-18 for different data batch sizes in seconds/image. The Time axis is log scaled.

Fig. 12: Computational complexity of EDropout with respect to the number of inference calls and inference time per image.

for N_{epoch} number of epochs and N_{batch} number of iterations, the upper bound for the number of inference calls (i.e. performing inference) is $S \cdot N_{epoch} \cdot N_{batch}$, that is S times more than one inference per training iteration, as demonstrated in Figure 12(a) for 200 training epochs. However, the benefit of this expense is the added diversity in searching for the sub-network with lower energy. Since the candidate states in the population are independent, one of the solutions is to implement the optimizer in parallel as a state vector level with shared memory (the population). Table V shows the inference time comparison between original models and EDropout per image in seconds. Assuming the inference time of a model as T_{model} , the results show $T_{EDropout} < S \cdot T_{Original}$ for $s \in \{8, 32\}$, which satisfies the above upper boundary. The parallel implementation of EDropout shows dramatic reduction in the inference time, and close to the original model.

It is obvious that increasing the data batch size for each iteration can also decrease the training time. As an example using ResNet-18, Figure 12(b) shows that increasing the batch size can decrease the training and inference time. Another method to reduce the execution time is using the concept of early state convergence, where the number of iterations for sub-network exploration can be defined or adaptively set by the model according to (11), as discussed in III-C4.

V. CONCLUSIONS

In this paper, we introduce the concept of energy-based dropout and pruning in deep neural networks. We propose a new method for partial training of deep neural networks (DNNs) based on the concept of dropout. An energy model

is proposed to compute energy loss of a population of binary candidate pruning state vectors, where each vector represents a sub-network of the DNN. An evolutionary technique searches the population of state vectors, selects the state vector with lowest energy loss in that iteration, and trains the corresponding sub-network using back-propagation. Ultimately, the states can converge to a *best state* and the algorithm continues fine-tuning the corresponding sub-network, which is equivalent to *pruning* of the DNN. One of the advantages of this method is capability of adding any type of constraint to the energy function and the evolution phase of candidate states without need for normalization, for any size DNN. The natural characteristic of the optimizer is the parallel structure, so that parallel computing methods can easily be implemented for the sake of faster optimization.

VI. ACKNOWLEDGMENT

The authors acknowledge financial support and access to the Digital Annealer (DA) of Fujitsu Laboratories Ltd. and Fujitsu Consulting (Canada) Inc.

REFERENCES

- [1] S. Han, H. Mao, and W. J. Dally, "Deep compression: Compressing deep neural networks with pruning, trained quantization and huffman coding," *arXiv preprint arXiv:1510.00149*, 2015.
- [2] N. Srivastava, G. Hinton, A. Krizhevsky, I. Sutskever, and R. Salakhutdinov, "Dropout: a simple way to prevent neural networks from overfitting," *The Journal of Machine Learning Research*, vol. 15, no. 1, pp. 1929–1958, 2014.
- [3] T. Hastie, R. Tibshirani, and M. Wainwright, *Statistical learning with sparsity: the lasso and generalizations*. CRC press, 2015.
- [4] J. Ba and B. Frey, "Adaptive dropout for training deep neural networks," in *Advances in Neural Information Processing Systems*, 2013, pp. 3084–3092.
- [5] D. P. Kingma, T. Salimans, and M. Welling, "Variational dropout and the local reparameterization trick," in *Advances in Neural Information Processing Systems*, 2015, pp. 2575–2583.
- [6] S. Park, J. Park, S.-J. Shin, and I.-C. Moon, "Adversarial dropout for supervised and semi-supervised learning," in *Thirty-Second AAAI Conference on Artificial Intelligence*, 2018.
- [7] L. Wan, M. Zeiler, S. Zhang, Y. Le Cun, and R. Fergus, "Regularization of neural networks using dropout," in *International conference on machine learning*, 2013, pp. 1058–1066.
- [8] A. Labach, H. Salehinejad, and S. Valaee, "Survey of dropout methods for deep neural networks," *arXiv preprint arXiv:1904.13310*, 2019.
- [9] Y. LeCun, J. S. Denker, and S. A. Solla, "Optimal brain damage," in *Advances in neural information processing systems*, 1990, pp. 598–605.
- [10] Z. Liu, M. Sun, T. Zhou, G. Huang, and T. Darrell, "Rethinking the value of network pruning," *arXiv preprint arXiv:1810.05270*, 2018.
- [11] S. J. Nowlan and G. E. Hinton, "Simplifying neural networks by soft weight-sharing," *Neural computation*, vol. 4, no. 4, pp. 473–493, 1992.
- [12] K. Ullrich, E. Meeds, and M. Welling, "Soft weight-sharing for neural network compression," *arXiv preprint arXiv:1702.04008*, 2017.
- [13] H. Salehinejad and S. Valaee, "Ising-dropout: A regularization method for training and compression of deep neural networks," in *ICASSP 2019-2019 IEEE International Conference on Acoustics, Speech and Signal Processing (ICASSP)*. IEEE, 2019, pp. 3602–3606.
- [14] S. Matsubara, H. Tamura, M. Takatsu, D. Yoo, B. Vatankehghadim, H. Yamasaki, T. Miyazawa, S. Tsukamoto, Y. Watanabe, K. Takemoto *et al.*, "Ising-model optimizer with parallel-trial bit-sieve engine," in *Conference on Complex, Intelligent, and Software Intensive Systems*. Springer, 2017, pp. 432–438.
- [15] H. Salehinejad, Z. Wang, and S. Valaee, "Ising dropout with node grouping for training and compression of deep neural networks," in *2019 IEEE Global Conference on Signal and Information Processing (GlobalSIP)*. IEEE, 2019, pp. 1–5.
- [16] Y. LeCun, S. Chopra, R. Hadsell, M. Ranzato, and F. Huang, "A tutorial on energy-based learning," *Predicting structured data*, vol. 1, no. 0, 2006.

- [17] K. V. Price, "Differential evolution," pp. 187–214, 2013.
- [18] S. Anwar, K. Hwang, and W. Sung, "Structured pruning of deep convolutional neural networks," *ACM Journal on Emerging Technologies in Computing Systems (JETC)*, vol. 13, no. 3, pp. 1–18, 2017.
- [19] W. Grathwohl, K.-C. Wang, J.-H. Jacobsen, D. Duvenaud, M. Norouzi, and K. Swersky, "Your classifier is secretly an energy based model and you should treat it like one," *arXiv preprint arXiv:1912.03263*, 2019.
- [20] A. Labach and S. Valaee, "A framework for neural network pruning using gibbs distributions," *arXiv preprint arXiv:2006.04981*, 2020.
- [21] G. Hinton, O. Vinyals, and J. Dean, "Distilling the knowledge in a neural network," *arXiv preprint arXiv:1503.02531*, 2015.
- [22] D. Barber and A. Botev, "Dealing with a large number of classes—likelihood, discrimination or ranking?" *arXiv preprint arXiv:1606.06959*, 2016.
- [23] R. M. Neal, "Annealed importance sampling," *Statistics and computing*, vol. 11, no. 2, pp. 125–139, 2001.
- [24] H. Salehinejad, S. Rahnamayan, and H. R. Tizhoosh, "Micro-differential evolution: Diversity enhancement and a comparative study," *Applied Soft Computing*, vol. 52, pp. 812–833, 2017.
- [25] K. P. Murphy, *Machine learning: a probabilistic perspective*. MIT press, 2012.
- [26] K. Dabiri, M. Malekmohammadi, A. Sheikholeslami, and H. Tamura, "Replica exchange mcmc hardware with automatic temperature selection and parallel trial," *IEEE Transactions on Parallel and Distributed Systems*, vol. 31, no. 7, pp. 1681–1692, 2020.
- [27] J. Lampinen, I. Zelinka *et al.*, "On stagnation of the differential evolution algorithm," in *Proceedings of MENDEL*, 2000, pp. 76–83.
- [28] H. Xiao, K. Rasul, and R. Vollgraf. (2017) Fashion-mnist: a novel image dataset for benchmarking machine learning algorithms.
- [29] T. Clanuwat, M. Bober-Irizar, A. Kitamoto, A. Lamb, K. Yamamoto, and D. Ha. (2018) Deep learning for classical japanese literature.
- [30] A. Krizhevsky, G. Hinton *et al.*, "Learning multiple layers of features from tiny images," 2009.
- [31] M.-E. Nilsback and A. Zisserman, "Automated flower classification over a large number of classes," in *2008 Sixth Indian Conference on Computer Vision, Graphics & Image Processing*. IEEE, 2008, pp. 722–729.
- [32] T. DeVries and G. W. Taylor, "Improved regularization of convolutional neural networks with cutout," *arXiv preprint arXiv:1708.04552*, 2017.
- [33] A. Krizhevsky, I. Sutskever, and G. E. Hinton, "Imagenet classification with deep convolutional neural networks," in *Advances in neural information processing systems*, 2012, pp. 1097–1105.
- [34] F. N. Iandola, S. Han, M. W. Moskewicz, K. Ashraf, W. J. Dally, and K. Keutzer, "Squeezenet: Alexnet-level accuracy with 50x fewer parameters and; 0.5 mb model size," *arXiv preprint arXiv:1602.07360*, 2016.
- [35] K. He, X. Zhang, S. Ren, and J. Sun, "Deep residual learning for image recognition," in *Proceedings of the IEEE conference on computer vision and pattern recognition*, 2016, pp. 770–778.
- [36] G. Hinton, N. Srivastava, and K. Swersky, "Neural networks for machine learning lecture 6a overview of mini-batch gradient descent," *Cited on*, vol. 14, no. 8, 2012.
- [37] M. D. Zeiler, "Adadelata: an adaptive learning rate method," *arXiv preprint arXiv:1212.5701*, 2012.
- [38] A. Paszke, S. Gross, F. Massa, A. Lerer, J. Bradbury, G. Chanan, T. Killeen, Z. Lin, N. Gimelshein, L. Antiga, A. Desmaison, A. Kopf, E. Yang, Z. DeVito, M. Raison, A. Tejani, S. Chilamkurthy, B. Steiner, L. Fang, J. Bai, and S. Chintala, "Pytorch: An imperative style, high-performance deep learning library," in *Advances in Neural Information Processing Systems 32*. Curran Associates, Inc., 2019, pp. 8024–8035.
- [39] F. N. Iandola, S. Han, M. W. Moskewicz, K. Ashraf, W. J. Dally, and K. Keutzer, "Squeezenet: Alexnet-level accuracy with 50x fewer parameters and; 0.5mb model size," *arXiv preprint arXiv:1602.07360*, 2016.